Journal of Renewable Materials
DOI:10.32604/jrm.2020.010215
Article

Tech Science Press

Dielectric Permittivity of Rigid Rapeseed Oil Polyol Polyurethane Biofoams and Petrochemical Foams at Low Frequencies

Ilze Beverte[1,*], Vairis Shtrauss[1], Aldis Kalpinsh[1], Uldis Lomanovskis[1], Ugis Cabulis[2], Irina Sevastyanova[2] and Sergejs Gaidukovs[3]

[1]Institute for Mechanics of Materials, University of Latvia, Riga, LV-1006, Latvia
[2]Latvian State Institute of Wood Chemistry, Riga, LV-1006, Latvia
[3]Faculty of Materials Science and Applied Chemistry, Institute of Polymer Materials, Institute of Applied Chemistry, Riga Technical University, Riga, LV-048, Latvia
*Corresponding Author: Ilze Beverte. Email: Ilze.Beverte@lu.lv
Received: 16 February 2020; Accepted: 20 May 2020

Abstract: Early investigations of dielectric permittivity of rigid polyurethane foams at low frequencies were made on petrochemical-origin foams, mainly by means of parallel plate capacitors. In the present investigation biopolyol was synthesized from Latvia-grown rapeseeds' oil by the transesterification method with triethanolamine, in an environmentally friendly process, without emission of harmful substances, at temperatures 175°C ± 5°C. Rigid, closed-cell rapeseed oil polyol polyurethane biofoams and petrochemical foams were made ensuring content of the renewable rapeseed oil polyol in ready foams 27 wt.%–29 wt.%. Dielectric permittivity of the polyurethane foams and the underlying monolithic petrochemical-origin polyurethane and biopolyurethane was measured with a non-destructive dielectric spectrometer equipped with a capacitive sensor of one-side access type at 16 discrete frequencies distributed geometrically over the band 10 Hz, … , 330 kHz. Permittivity value of the gaseous phase in the closed-cells was estimated to be $\varepsilon_g \approx 1.001$ that corresponds to the values, characteristic for the most of gases. Dielectric permittivity of petrochemical polyurethane foams and the mentioned biofoams was compared with permittivity of polyurethane foams from industrial producers *Sika JSC* and *General Plastics Manufacturing Co*. Polyurethane foams of the developed formulation exhibit competitive, low dielectric permittivity, not exceeding that of the foams from industrial producers: petrochemical foams up to 550 kg/m^3 and the mentioned biofoams, comprising the renewable rapeseed oil polyol, up to densities 230–250 kg/m^3. Considering petrochemical-origin polyurethane foams as a heterogeneous media "Polymer—gaseous phase", the applicability of the rule of mixture and Maxwell–Garnett equation to model mathematically the dependence of effective dielectric permittivity on the volume fraction of phases was showed.

Keywords: Polyurethane foams; rapeseed oil polyol; biofoams; dielectric permittivity; capacitive sensor; one-side access; low frequencies

1 Introduction

Rigid polyurethane (PUR) foams [1] due to their outstanding thermal insulation properties and acceptable load bearing capacity have gained widespread applications in many sectors of economy, such as construction: sandwich structures and panels, thermal insulation of mortars for masonry, manufacturing industry: electric insulation in electronics, equipment housing and components, transport: cooling vans, vehicle insulation, thermal insulation of cryogenic tanks in space vehicles, emergency shock absorbers, other community services: both heat and cold saving insulation in stores, warehouse buildings and constructions etc. The additional advantages of PUR foams come from their non-corrosiveness, low dielectric permittivity, recyclability and good moisture resistance [2]. Light-weight rigid PUR foams have low dielectric interference, their dielectric permittivity is non-dispersive, and so a complete dielectric performance can be quarantined at every frequency range. That makes rigid, closed-cell, light-weight PUR foams to be an appropriate material for aerospace and automotive components, electronics packaging, electric insulators, radomes (Protective structures for out-door telescopes, locators, antennas etc.), providing a radio-frequency transparent layer along dimensional stability.

At present the main raw materials used for the production of polyurethane foams are products of petrochemical origin [2,3]. The Earth oil resources are limited, un-renewable, expensive and available not in all countries; their depletion in the nearest future is prognosticated. Consequently, the prices of petrochemical raw materials are becoming increasingly unstable. Latvia and other countries without their own oil resources have to acquire each petrochemical component from outside, at high costs. Raw materials from bioresources represent an abundant, renewable and low cost resource that could play an alternative role to petrochemical resources. Synthesis of polymers from such materials is widely investigated by leading research groups in different countries [3–7]. In the last decades, PUR industry has shown an increasing interest in polyols, derived from different types of bio-oils [8–9]. The liquefaction of lignocellulosic biomass has been also widely studied for synthesis of polyols [10], thus the polysaccharides as well serve as raw materials for polyols [11]. These biobased components can be successfully used to obtain different types of PUR materials, including rigid PUR-polyisocyanurate foams [12,13] and flexible PUR foams [14]. In [6] three different approaches for polyol synthesis from rapeseed oil are considered and the acquired rapeseed oil biopolyols are used in production of rigid polyisocyanurate biofoams [15].

As non-metallic materials, widely applied in industry, PUR foams require efficient, nondestructive evaluation (NDE) methods for controlling the quality of manufactured materials and items. In NDE for non-metallic materials, in the frequency band up to 10 MHz, capacitance method is one of the main testing methods [16]. In direct way the capacitance method enables to determine dielectric properties of a material, such as the real and imaginary part of dielectric permittivity, their dependence on frequency and temperature, relaxation parameters, etc. [17]. Knowledge on dielectric permittivity of rigid PUR foams is necessary in NDE, in practical applications, related to electromagnetic field etc.

Potential of the method was significantly increased with developing one-side access (OSA) capacitive sensors [18,19] allowing NDE by applying the sensor merely to one side of the testing object (A bulk material or a product), without making testing samples, thus sparing time, labor and finance. At present OSA capacitive sensors are widely used in proximity/displacement measurements, intelligent human interfacing, non-destructive testing, material characterization, determination of thickness of non-metallic materials, in security systems etc. [19–23]. At the same time there is no data about investigation of rigid PUR foams' dielectric permittivity with OSA capacitive sensor method.

Scientific et al. information search showed a shortage of systematic, reliable experimental data of permittivity of rigid PUR foams in the characteristic range of densities 30–1280 kg/m^3, at frequencies < 10 MHz, even if acquired with other methods, e.g., the destructive ones, using parallel-plate capacitors. The technical difficulties, caused by the PUR foams themselves are connected to the extremely low permittivity values, e.g., at density 31 kg/m^3 permittivity $\varepsilon \approx 1.065$ (1 kHz), only ≈ 6% higher than the permittivity of vacuum. Some permittivity values are reported in an experimental investigation of rigid petrochemical PUR

foams with a parallel plate capacitor at two frequencies 100 Hz and 10 MHz according to ASTM D1673 [24] and at 1 kHz, 10 kHz, 0.1 MHz and 1 MHz according to ASTM D150-94 [25]. Practically no dielectric permittivity data is available for rigid rapeseed oil polyol PUR biofoams and for monolithic PUR-s, both petrochemical and biopolyurethane. Results provided by mathematical models of effective dielectric properties of composite materials [17,24,26,27] are investigated insufficiently in application to rigid PUR foams.

The given interdisciplinary research investigates dielectric permittivity spectra of (a) Rigid rapeseed oil polyol PUR biofoams (Further—PUR biofoams) and petrochemical PUR foams in a wide range of densities, including very low ones 30–50 kg/m^3 and (b) Corresponding PUR monoliths (Biopolyurethane and petrochemical PUR) in an innovative way—with a OSA capacitive sensor method. To our best knowledge the scientific information sources comprise no data about research of rigid PUR foams' dielectric permittivity with OSA capacitive sensor method. For the first time dielectric permittivity of the mentioned polymeric materials (a) and (b) is determined at 16 discrete frequencies, increasing in a geometric progression over the band 10 Hz, 20 Hz, … , 327 680 Hz experimentally and theoretically. Experimental part of the research is performed by means of a NDE dielectric spectrometer equipped with a capacitive sensor of one-side access type realising an innovative, stray-immune measuring technology, developed in [18,23]. Influence of the biobased polyol on permittivity of rigid PUR foams and monolithic PUR is evaluated based on the acquired experimental data. Considering rigid PUR foams as a "Polymer—gaseous phase" composite, effective permittivity is calculated according to three different mathematical models of composite materials, the numerical results are compared to the acquired experimental data and new conclusions are made.

2 Experimental

2.1 Raw Materials

To make rigid closed-cell PUR foams, the following raw materials were used as purchased: polyether-type polyols Lupranol 3300; Lupranol 3422 (*BASF*); Voranol RA640 (*DOW*) and Ixol B251 (*Solvay*), polyester-type polyol Lupraphen 1901/1 (*BASF*); crosslinking agent Quadrol (*BASF*); chain extender diethylene glycol (*Sigma Aldricht*); flame retardant Tris(1-chloro-2-propyl)phosphate (TCPP) (*Albermarle*); surfactant Silicone L6915LV (*Momentive*); catalysts PC CAT NP10 (*Air Products*) and Kosmos 19 (*Evonik*); pentane—a physical blowing agent, permitted in the European Union and a chemical blowing agent—distilled water. Desmodur® 44V20L (*Bayer*) was used as a polyisocyanate component for all rigid PUR foams formulations. It is a solvent-free product based on 4,4'-diphenylmethane diisocyanate (MDI) and contains oligomers of high functionality. The average functionality was 2.8 to 2.9 and the NCO content was 30.5 wt.%–32.5 wt.%. Isocyanate indexes for rigid PUR foams II = 130, thus the amount of necessary MDI was adjusted to compensate water accordingly and was in range from 147 pbw to 170 pbw.

Biopolyol was synthesized from Latvia-grown rapeseeds' oil by the transesterification method with triethanolamine (molar ratios 1 M:2.5 M and 1 M:2.9 M), in an environmentally friendly process, without emission of harmful substances, at temperatures T = 175°C ± 5°C [6]. The obtained biopolyol (Fig. 1) contains 1 M glycerol and 3 M triethanolamine esters which comprise saturated and unsaturated fatty acid radicals with carbon chain length C16–C18. Fatty acid radicals will act as dangling chains in the obtained PUR biofoams. Polyols obtained from rapeseed oil transesterification reaction with triethanolamine showed potential to be used in rigid PUR biofoams as their mechanical characteristics improved, especially in cases with the increase of isocyanate index [28].

Rigid, closed-cell PUR biofoams were made according to formulation in Tab. 1, ensuring content of the renewable rapeseed oil polyol in ready foams 27 wt.%–29 wt.%. As the aim of the research is making and testing of building thermal insulation PUR foams materials, their biodegradability is not a requirement.

2.2 PUR Foams' Blocks

Rigid closed-cell petrochemical PUR foams were made in a range of apparent core density 32 kg/m^3 $\leq \rho_f \leq$ 540 kg/m^3 in blocks, in (a) open free-rise moulds (25 cm × 25 cm × 20 cm) and in (b) closed cylindrical polypropylene moulds of height 8.0 and inner diameter 10.0 cm, Fig. 2. Rigid closed-cell biopolyurethane

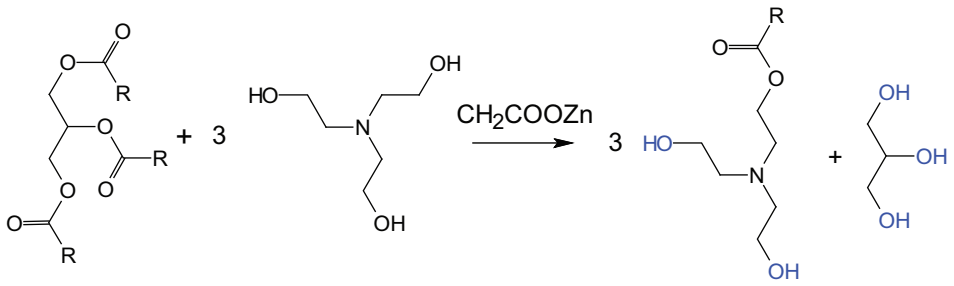

Figure 1: Idealised rapeseed oil transesterification with triethanolamine in presence of zinc acetate catalyst [29]

Table 1: Formulations of rigid PUR foams

N	Component, pbw*	Formulation	
		Petrochemical	Renewable
1	Biopolyol	–	80
2	Polyether polyols	45	15
3	Polyester polyol	30	–
4	Crosslinking agent	–	5
5	Chain extender	25	–
6	Flame retardant	15	20
7	Surfactant	1.5	2.0
8	Catalyst package	0.3	1.6
9	Physical blowing agent	40–25	–
10	Chemical blowing agent	1.5–0.1	1.0–0.1
11	Polyisocyanate	168	170–147
Densities of rigid PUR foams, kg/m^3:			
	Blowing agent—pentane	32–80	–
	Blowing agent—water	81–540	80–450
Renewable polyol content in ready foams, wt.%		–	27–29

*Parts by weight per hundred parts of polyol.

(a) (b)

Figure 2: Blocks made in (a) rectangular and (b) cylindrical moulds

foams were made in a range of apparent core density 80 kg/m^3 ≤ ρ_f ≤ 450 kg/m^3. Apparent core density of the both types of PUR foams (Further—density) was determined according to ISO 845:2006. Difference in densities was achieved by varying the amount of physical or chemical blowing agents, Tab. 1.

For PUR blocks making in lab conditions the system cannot be too fast, i.e., the cream time has to be 15–30 s. To obtain PUR foams' polyols' composition, components were weighted on lab scales and mixed by mechanical stirrer gradually for 30–60 s each. After all components of the composition were added, the polyols' system was conditioned for 24 h at room temperature in a sealed container to separate air that has been mixed in. To obtain rigid PUR foams blocks, the polyols' component and MDI were mixed with mechanical stirrer (2400 rpm ± 20 rpm) for 10 s and poured into a closed mould. The polymerization reaction took place at room temperature for all the obtained blocks and was completed in ca. 30–45 min.

To estimate closed-cell foams' porosity, mass of gas m_g in a unit volume of foams can be considered as insignificant in comparison to the mass of monolithic polymer m_p:

$$m_f = m_p + m_g;\ m_g \ll m_p \text{ and } m_f \approx m_p, \tag{1}$$

where m_f—mass of foams in the unit volume. Volume fractions of monolithic polymer (Space filling coefficient) and gas (Porosity) in volume of foams V_f can be expressed as:

$$\eta_p = V_p/V_f = (m_p/\rho_p)/(m_f/\rho_f) = \rho_f/\rho_p;$$

$$\eta_g = V_g/V_f = (V_f - V_p)/V_f = 1 - V_p/V_f = 1 - \rho_f/\rho_p; \tag{2}$$

where V_f and V_p—volume of foams and monolithic polymer. For petrochemical PUR foams' of Tab. 1 formulation and densities 32 kg/m^3 ≤ ρ_f ≤ 540 kg/m^3 porosity 97.5% ≥ η_g ≥ 57.8%. For biopolyurethane foams of Tab. 1 formulation and densities 80 kg/m^3 ≤ ρ_f ≤ 450 kg/m^3 porosity 93.0% ≥ η_g ≥ 60.9%.

Industrially manufactured rigid petrochemical origin PUR foams from a European producer *Sika JSC* and *General Plastics Manufacturing company* (LAST-A-FOAM® series), the United States of America, were investigated as well. Results of the four groups of PUR foams were compared and conclusions made.

2.3 Monolithic Polyurethane

To make monolithic petrochemical PUR and biopolyurethane, the liquid mixture of the corresponding formulation that provided foams of density ≈ 40 kg/m^3 was poured in polyethylene (PET) ampoules of inner diameter ≈ 15 mm and length 80 mm [15]. No foaming agent was added. The ampoules were centrifuged for 15 min at 5500 rpm in a centrifuge Hettich EBA-20 (*Andreas Hettich GmbH & Co. KG*) to eliminate air inclusions created by mechanical mixing. The other batch of monolithic PUR rods was made on centrifuge Sigma 3-30KS (*Sigma Laborzentrifugen GmbH*) by processing ampoules of inner diameter 25.4 mm, length 115 mm with liquid formulation for 20 min at 5000 rpm, Fig. 3.

The PUR rods were removed from ampoules and samples made. The developed technology ensured ≈ 2/3 of the length of cylindrical part free from gaseous inclusions for the petrochemical PUR and ≈ 1/3 for biopolyurethane. The average density of petrochemical monolithic PUR cylinders of diameter ≈ 14 mm was determined as ρ_p = 1286 kg/m^3 and that of samples of diameter ≈ 25.4 mm as ρ_p = 1274 kg/m^3. Further it is assumed ρ_p = 1280 kg/m^3. The density value is in a good correspondence with values reported elsewhere [1,15,30]. The average density of monolithic biopolyurethane cylinders, diameter ≈ 25.4 mm, comprising Latvia-grown rapeseeds' oil polyol as a component, was determined to be ρ_p = 1150 kg/m^3.

2.4 Dielectric Permittivity

Dielectric permittivity of the PUR foams was measured with a NDE dielectric spectrometer equipped with a capacitive sensor of one-side access (OSA) type, diameter of the annular outer electrode D_0 =

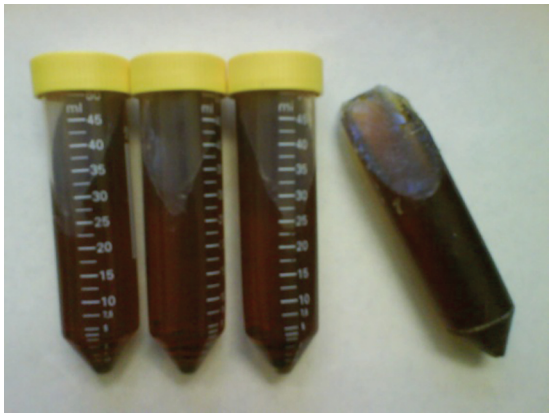

Figure 3: PET ampoules (D_{in} = 25.4 mm) with hardened, monolithic petrochemical PUR and a PUR rod

43 mm [23]. The capacitive sensor of OSA type was pushed against one surface of a non-destructible test object —the sample. The sample was excited via electrodes, by electrical field generated by sinusoidal voltage signals from a multi-frequency generator of spectrometer. Amplitude value of the sinusoidal excitation signals U_0 = 20 V. The signals were generated at discrete frequencies, increasing in a geometric progression [23]:

$$f_n = f_0,\ 2f_0,\ \ldots,\ 2^{(n-1)}f_0\ \text{Hz};$$

$$f = 10\ \text{Hz},\ 20\ \text{Hz},\ \ldots,\ 327\ 680\ \text{Hz}, \tag{3}$$

where f_0 = 10 Hz and the ordeal number of frequency n = 1, 2, … , 16.

The dielectric permittivity spectra of rigid PUR foams ε_f of the given formulation, Tab. 1, were determined experimentally for the signal frequencies of Eq. (3) in dependence of foams' density; in density range 32–540 kg/m^3. Permittivity was measured on cylindrical samples of height h = 20 mm and diameter D = 45 mm. Density in direct vicinity to the sample's contact surface with the sensor may be different from the calculated average density attributed to the whole sample. A density gradient may exist in the molded foams' blocks along rise direction, especially in free rise [31,32]. To reduce that impact, samples were picked from the most homogeneous parts of the blocks. Air gaps between active surface of the sensor and the sample may reduce the measured value of permittivity [17–23,33–35] therefore surfaces of the samples were processed to ensure an appropriate degree of smoothness. Triboelectricity that accumulated on the samples while grinding the sides was channeled away by placing samples on a conductive, grounded surface. Prior to permittivity measurements the samples were conditioned by storing them at temperature T = 21°C ± 1°C and relative humidity RH = 45% ± 5% for a minimum of 24 h. Three successive measurements of permittivity spectrum were made for each sample, for one and the same surface. Fig. 4 comprises dielectric spectra at densities (a) 32.1 kg/m^3, (b) 48.3 kg/m^3, (c) 63.0 kg/m^3, (d) 73.5 kg/m^3, (e) 80.1 kg/m^3 and (f) 89.1 kg/m^3 and Fig. 5—at densities (a) 101.1 kg/m^3, (b) 182.3 kg/m^3, (c) 324.8 kg/m^3, (d) 406.4 kg/m^3 and (e) 509.0 kg/m^3. Each spectrum $\varepsilon_f = \varepsilon_f(f_n)$ is a result of averaging over three successive measurement data.

In the density range 32–89 kg/m^3 the permittivity values are $1.052 \le \varepsilon_f \le 1.165$ and in the range 102–509 kg/m^3 $1.153 \le \varepsilon_f \le 1.190$. At a fixed density ρ_f = const. the frequency f_1 = 10 Hz provides the highest value of ε_f and the frequency f_{16} = 0.33 MHz—the lowest.

Fig. 6 comprises permittivity spectra of PUR biofoams at densities (a) 81.2 kg/m^3, (b) 107.8 kg/m^3, (c) 147.6 kg/m^3, (d) 190.1 kg/m^3, (e) 365.8 kg/m^3 and (f) 442.4 kg/m^3. For both petrochemical PUR foams and

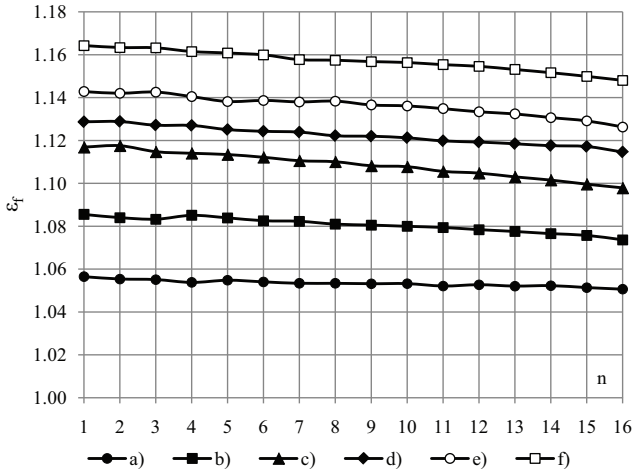

Figure 4: Permittivity spectra of PUR foams at densities 32.1–89.1 kg/m^3

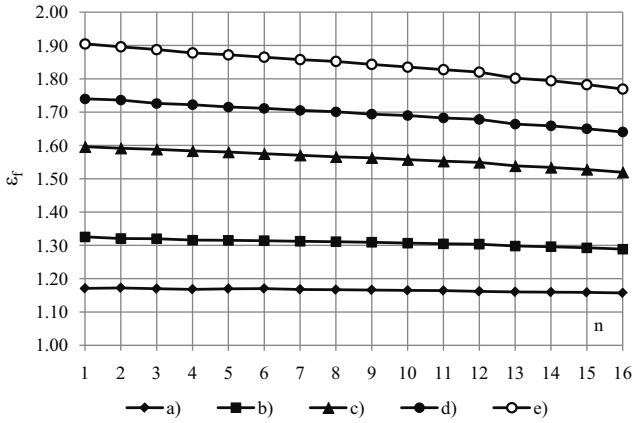

Figure 5: Permittivity spectra of PUR foams at densities 101.1–509.0 kg/m^3

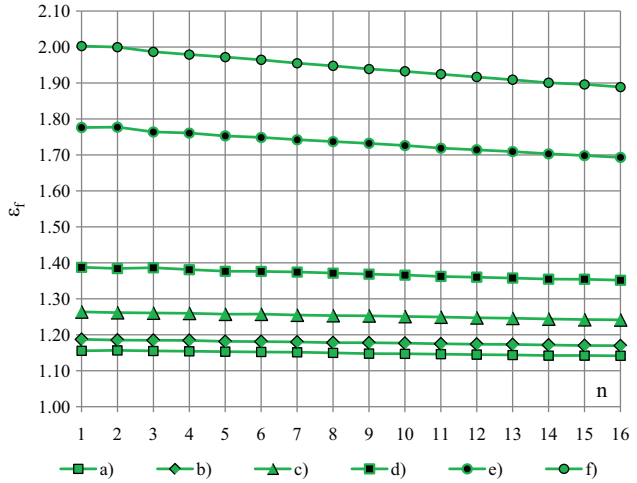

Figure 6: Permittivity spectra of PUR biofoams at densities 81.2–442.4 kg/m^3

PUR biofoams the absolute value of standard deviation over permittivity values in three successive measurements at all densities remains less than 1%.

Permittivity values measured with the OSA capacitive sensor were compared to those measured on samples made from the same PUR foams with a Broadband Dielectric Spectrometer BDS-50 (*Novocontrol Technologies GmbH & Co. KG*), comprising a parallel plate capacitor. Petrochemical PUR foams of densities 95, 152 and 222 kg/m^3 and corresponding monolithic PUR, density 1280 kg/m^3, were tested. The relative difference between data provided by the two methods/apparatuses remains less than ≈ 5% that proves high accuracy of OSA capacitive sensor. Fig. 7 gives examples of permittivity spectra measured with two methods/apparatuses for petrochemical PUR foams of density (1) 95 kg/m^3; 1-a: OSA capacitive sensor, 1-b: spectrometer BDS-50 and (2) 222 kg/m^3; 2-a: OSA capacitive sensor, 2-b: spectrometer BDS-50.

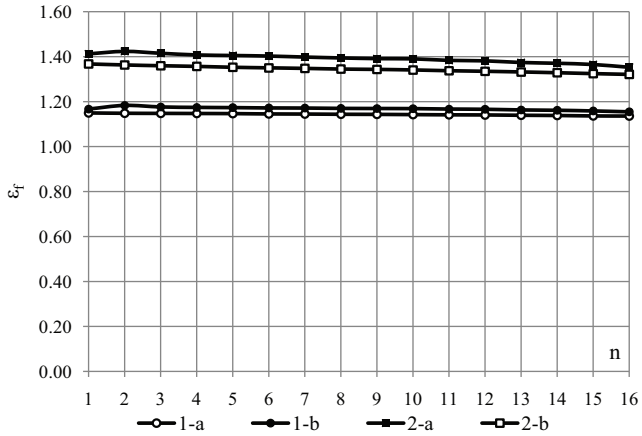

Figure 7: Permittivity spectra of petrochemical PUR foams, density 95 and 222 kg/m^3

2.5 Dropping Factor

Dielectric dispersion is the dependence of permittivity of a dielectric material on the frequency of an applied electric field. Because there is a lag between changes in the external electric field and changes in polarization in a dielectric, permittivity of a dielectric is a complicated function of frequency of the electric field [16,33]. Since the polarization and relaxation mechanisms of PUR foams at low frequencies are not yet sufficiently investigated, a normalized dropping factor of dielectric permittivity over an 11-octave frequency band is implemented to characterize the difference between permittivity of PUR foams at different frequencies. Some relatively small fluctuations of permittivity from the trendline of a spectrum were observed at frequencies f_1, f_2 and f_{15}, f_{16} therefore the dielectric spectra were approximated with the third order polynomials and F values were calculated from the most monotonous part f_3, f_4, … , f_{14} (40, 80, … , 81 920 Hz) of the approximated spectra as:

$$F = [\varepsilon_f(f_3) - \varepsilon_f(f_{14})]/\varepsilon_f(f_3), \tag{4}$$

where $\varepsilon_f(f_3)$ and $\varepsilon_f(f_{14})$—permittivity at f_3 and f_{14}. Fig. 8 gives the dropping factor at densities 32–540 kg/m^3 for Tab. 1 formulations: (a) petrochemical origin PUR foams and (b) PUR biofoams according to calculations from experimental data as well as the corresponding trendlines. It can be seen that even at densities 400–500 kg/m^3 the F values of both types of the investigated rigid closed-cell PUR foams does not exceed 5.0%–5.5%. PUR biofoams comprising the rapeseed oil polyol, exhibit a dropping factor only ≈ 0.5%–1.0% higher that the petrochemical ones.

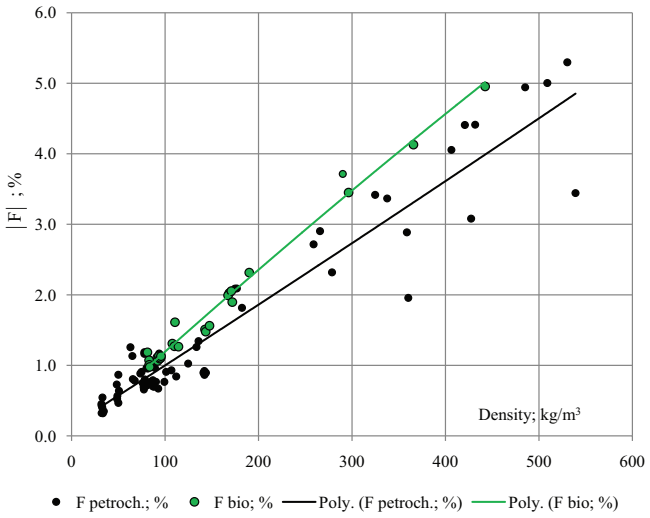

Figure 8: Dropping factor F, % of rigid PUR foams

The dependence of PUR foams permittivity on density is given in Fig. 9 for densities 32 kg/m^3 ≤ ρ_f ≤ 1280 kg/m^3 at the lowest and the highest frequency f_1 = 10 Hz and f_{16} = 0.33 MHz, density 1280 kg/m^3 corresponding to the monolithic PUR polymer. The trendlines of experimental data $\varepsilon_f = \varepsilon_f(\rho_f)$ at other frequencies f_2, f_3, … , f_{15} lie inside the "Fork", formed by graphs at f_1 and f_{16}. The width of the "Fork" angle gives a measure of difference between polarization processes in the given PUR foams at different frequencies.

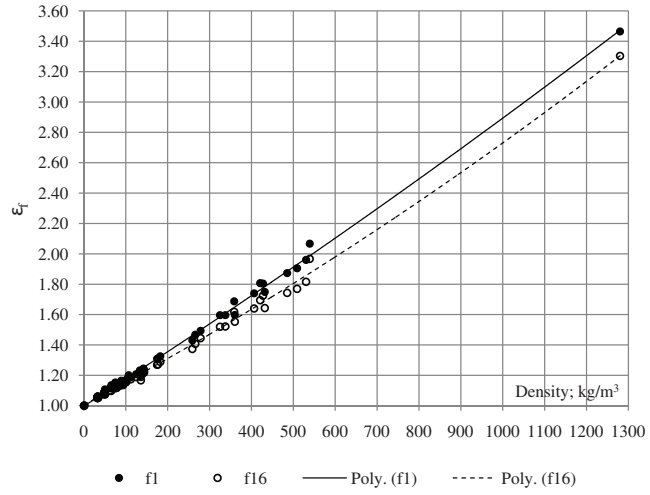

Figure 9: Permittivity of PUR foams in dependence of density 32 kg/m^3 ≤ ρ_f ≤ 1280 kg/m^3

The slightly non-linear dependence $\varepsilon_f = \varepsilon_f(\rho_f)$ can be well approximated by the least squares method, by a second order polynomial (In EXCEL):

$$\varepsilon_f = 0.00000013\rho_f^2 + 0.00176425\rho_f + 0.99696478;\ R^2 = 0.998 \text{ at } f_1 \text{ and}$$

$$\varepsilon_f = 0.00000025\rho_f^2 + 0.00147030\rho_f + 1.00558289;\ R^2 = 0.997 \text{ at } f_{16}, \quad (5)$$

where R^2—the coefficient of determination, giving a statistical measure of how close the experimental data are to the fitted regression line. The amount of significant figures after the decimal point that have to be

retained in the coefficients of approximating Eq. (5) is determined by the coefficient before the square member of the polynomial that may not become zero in order not to lose the non-linear character of the relationship $\varepsilon_f = \varepsilon_f(f_n)$. Numerical estimations proved that for the given PUR foams 7–8 significant figures have to be retained after the decimal point in the trendline equations to get theoretical curves, adequately modeling the experimental data trends.

The dependence $\varepsilon_f = \varepsilon_f(\rho_f)$ is given in Fig. 10 for the same experimental data, but in a smaller density range 32 kg/m^3 $\leq \rho_f \leq$ 200 kg/m^3. That corresponds to PUR foams of a relatively small space filling coefficient $\eta_p = \rho_f/\rho_p \leq 16\%$ and high porosity $\eta_g = 1 - \eta_p \geq 84\%$, useful mainly in thermal insulation ($\rho_f \leq 80$ kg/m^3) and building applications.

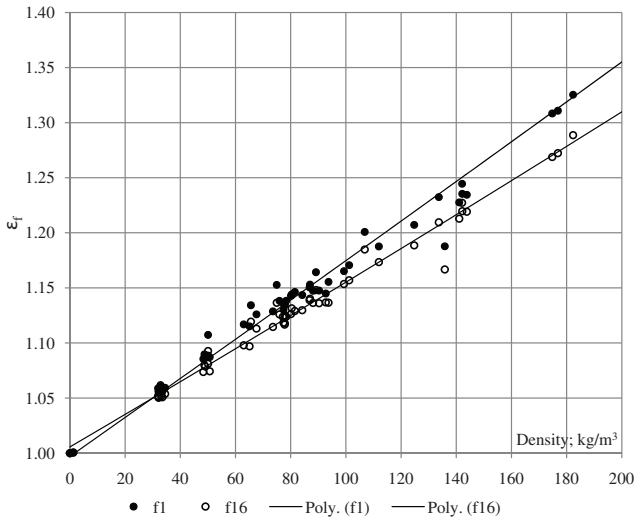

Figure 10: Permittivity of PUR foams in dependence of density $\rho_f \leq 200$ kg/m^3

2.6 PUR Foams from Different Producers

In order to position the PUR foams of Tab. 1 formulation, their permittivity properties were compared to those of PUR foams from industrial producers. Fig. 11 gives the permittivity spectra of rigid PUR foams from different producers, but of similar densities: *General Plastics Manufacturing Co*.—95 kg/m^3, *Sika JSC*—90 kg/m^3, Tab. 1 formulation petrochemical foams—88 kg/m^3 and Tab. 1 formulation PUR biofoams—81 kg/m^3. The overall character of the four spectra is similar: the shape, the values and the slope, characterized by the dropping factor. The relative difference between permittivity values of the four spectra is less than 3%.

To determine the functional dependence $\varepsilon_f = \varepsilon_f(\rho_f)$, experimental data of dielectric permittivity were approximated with (a) The third order polynomials over each permittivity spectrum corresponding to a definite density and then with (b) The second order polynomials at each frequency f_n, n = 1, 2, … , 16 over all tested foams' densities. Fig. 12 presents as an example the function $\varepsilon_f = \varepsilon_f(\rho_f)$ at a single frequency f_8 = 1280 Hz for rigid PUR foams of formulation in Tab. 1 (Petrochemical and biofoams) and for foams from industry-scale producers *Sika JSC* and *General Plastics Manufacturing Co*.

It can be seen from Fig. 12, that the trendlines of all four groups of rigid PUR foams, including PUR biofoams are coincidental up to densities 230–250 kg/m^3. PUR foams of Tab. 1 formulation exhibit comparable, low dielectric permittivity, not exceeding that of the foams from industrial producers: (a) Tab. 1 petrochemical PUR foams up to 550 kg/m^3 and (b) Tab. 1 PUR biofoams, comprising the renewable polyol, up to densities 230–250 kg/m^3. Above 230 kg/m^3 permittivity of PUR biofoams increases and at density 450 kg/m^3 is ≈ 10% higher than that of petrochemical foams. Dielectric

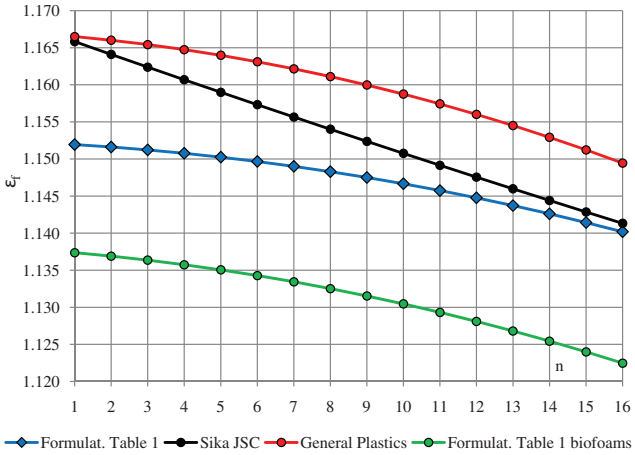

Figure 11: Permittivity spectra of PUR foams from different producers

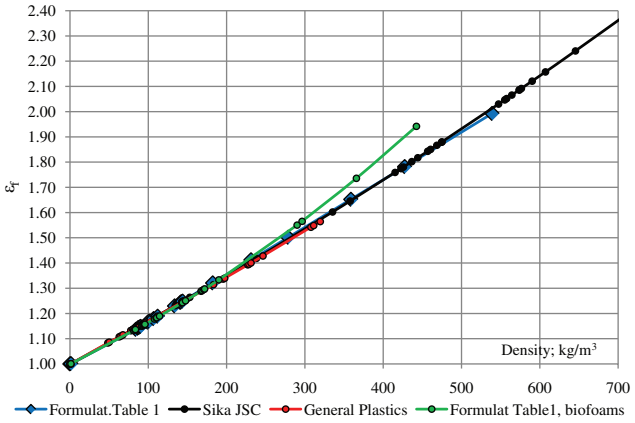

Figure 12: Permittivity of PUR foams from different producers; $f = f_8 = 1280$ Hz

permittivity of PUR biofoams, comprising the renewable, Latvia grown rapeseed oil polyol in ready foams 27 wt.%–29 wt.% remains comparable to that of petrochemical PUR foams up to 230–250 kg/m^3 at other frequencies of the spectrum (3) as well.

3 Theoretical

3.1 Rule of Mixture

To apply the rule of mixture [26,27] and calculate the dielectric permittivity of PUR foams, closed-cell foams are modeled as a two-phase composite consisting of a matrix of monolithic polymer and a gaseous dispersed phase. It is assumed that at each single frequency f_n the permittivity of foams is the volume-weighted average of the permittivity of phases:

$$\varepsilon_f(f_n) = \varepsilon_p(f_n)\eta_p + \varepsilon_g(f_n)\eta_g; n = 1,\ 2,\ \ldots,\ 16; \tag{6}$$

where $\varepsilon_p(f_n)$, $\varepsilon_g(f_n)$—permittivity of the monolithic PUR and gas in closed cells of the foams.

$$\text{When } \eta_g \to 0,\ \varepsilon_f(f_n) \to \varepsilon_p(f_n) \text{ and when } \eta_g \to 1,\ \varepsilon_f \to \varepsilon_g. \tag{7}$$

Then Eq. (6) can be expressed by densities of phases, Eq. (2):

$$\varepsilon_f(f_n) = \varepsilon_p(f_n)\rho_f/\rho_p + \varepsilon_g(f_n)(1 - \rho_f/\rho_p). \quad (8)$$

To determine the dependence $\varepsilon_f = \varepsilon_f(f_n)$, permittivity of monolithic PUR and of gaseous phase has to be measured or estimated.

3.2 Polymer Phase

Due to limited transversal and lateral dimensions of the monolithic PUR rods (Diameter ≈ 25 mm, length of the cylindrical part ≈ 60 mm), permittivity spectrums of monolithic petrochemical PUR and biopolyurethane were measured on two semi-cylindrical samples each. Two semi-cylinders were cut from a petrochemical PUR rod, ρ = 1280 kg/m^3 and two—from a biopolyurethane rod, ρ = 1150 kg/m^3. Side by side the two semi-cylinders form a round cylinder, height h = 12 mm, diameter D = 45 mm, fully covering the active surface of the sensor.

Prior to that an experiment was made where permittivity spectrum was first measured on a cylindrical sample, height h = 12 mm, diameter D = 45 mm, made of a non-porous PUR material Sika Block PUR M960 (*Sika JSC*) of similar density ρ = 1180 kg/m^3 and dielectric permittivity. Then the sample was cut along diameter in two equal semi-cylindrical parts, the parts were pushed together and fixed firmly with an elastic band along outer perimeter and permittivity was measured again. The same experiment was made for PUR foams of density 147.77 kg/m^3. For both materials, non-porous and porous, the results at each frequency f_n (Data at frequencies f_1, f_8 and f_{16} included as an example) showed small relative difference between permittivity values of the cylindrical and the two semi-cylindrical samples ε_c and ε_{sc}: $r = (\varepsilon_c - \varepsilon_{sc})/\varepsilon_c$; $|r| < 0.5\%$; Tab. 2.

Table 2: Permittivity of cylindrical and semi-cylindrical petrochemical samples

N	Material	Density; kg/m^3	Sample	h; mm	ε		
					f_1	f_8	f_{16}
1	PUR foams	148	A cylinder	12	1.266	1.246	1.224
2			Semi-cylinders		1.266	1.244	1.224
				r; %	0.00	0.16	0.00
3	Sika Block PUR M960	1180	A cylinder	12	3.748	3.672	3.507
4			Semi-cylinders		3.764	3.681	3.520
				r; %	– 0.43	– 0.25	– 0.37
5	Monolithic PUR	1280	Semi-cylinders	12	3.474	3.408	3.310

It can be expected that similar results will be acquired for monolithic PUR (Petrochemical and bio) and permittivity of a cylindrical sample will differ little from that of two semi-cylinders, Tab. 2.

To estimate influence of the limited height h = 12 mm of the monolithic PUR samples, penetration depth of electric field generated by the electrodes into a sample was investigated on the non-porous PUR material Sika Block PUR M960, density 1180 kg/m^3 and on PUR foams, density 50 and 147.77 kg/m^3. It was found that each of the mentioned materials provided practically equal values of permittivity for thicknesses of a sample h = 6–25 mm and higher. When thickness of a sample was reduced below h ≈ 5–6 mm, the permittivity value started to decrease. It was assumed that the height of the monolithic PUR sample h = 12 mm, two times higher than the limit height 6 mm, was sufficient to acquire reliable permittivity data.

The experimentally determined values of permittivity of monolithic petrochemical PUR polymer lie in limits $3.474 \geq \varepsilon_p \geq 3.310$ in the considered frequency range 10 Hz $\leq f_n \leq$ 0.33 MHz; Fig. 13a and dropping factor value F ≈ 6.2%. Permittivity values of monolithic biopolyurethane, comprising Latvia grown rapeseed oil polyol in a ready monoliths 27–29 wt.% are $3.413 \geq \varepsilon_{pb} \geq 3.100$ and F ≈ 6.9%. That permits to categorize both monolithic polyurethanes as polar synthetic plastics [36]. With frequency increasing the difference $\Delta\varepsilon = \varepsilon_p - \varepsilon_{pb}$ between permittivity of petrochemical PUR and biopolyurethane increases from $\Delta\varepsilon \approx 0.0$ at f_1 to $\Delta\varepsilon \approx 0.2$ at f_{16}. For comparison permittivity spectrum of the monolithic PUR from *Sika JSC*, density 1180 kg/m^3, was also determined experimentally, Fig. 13c. The spectrum of monolithic Sika PUR exhibits similar overall character and permittivity values: $3.748 \geq \varepsilon_p \geq 3.507$; F ≈ 4.1%.

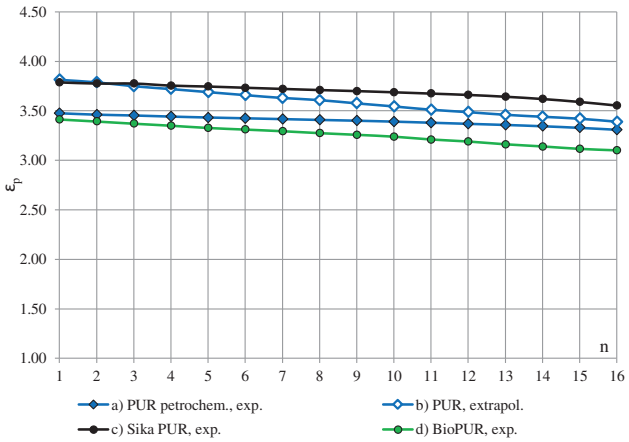

Figure 13: Permittivity spectra $\varepsilon_p = \varepsilon_p(f_n)$ of monolithic PUR-s

Permittivity values measured with the OSA capacitive sensor were compared to those measured on samples, made from the same PUR monoliths with the Broadband Dielectric Spectrometer BDS-50. The relative difference between data provided by the two methods/apparatuses remains less than ≈ 5%.

Permittivity spectrum of a monolithic PUR, e.g., —petrochemical, can be estimated also by extrapolation of the approximating functions of the experimental data points ε_f at each frequency to the density of monolithic polymer ρ_p = 1280 kg/m^3. The function $\varepsilon_f = \varepsilon_f(\rho_f)$ of the experimental data points for densities up to 540 kg/m^3, without the data of monolithic PUR is approximated by:

$$\varepsilon_f = 0.00000046\rho_f^2 + 0.00160996\rho_f + 1.00605267;\ R^2 = 0.996 \text{ at } f_1 \text{ and}$$

$$\varepsilon_f = 0.00000024\rho_f^2 + 0.00148184\rho_f + 1.00417122;\ R^2 = 0.993 \text{ at } f_{16}. \quad (9)$$

Calculations of the permittivity ε_p at ρ_p = 1280 kg/m^3 according to Eq. (9) provide values ≈ 2%–8% higher than the experimentally determined ones, Fig. 13b. Additional experimental data points would be necessary for medium to high density foams' ρ_f = 540–1280 kg/m^3 to increase the precision of extrapolation.

3.3 Gaseous Phase

To calculate permittivity of PUR foams $\varepsilon_f = \varepsilon_f(\rho_f)$, permittivity of the gaseous phase in closed cells of the given formulation has to be estimated. From the rule of mixture, Eq. (8) dielectric permittivity of monolithic PUR polymer can be expressed as:

$$\varepsilon_p(f_n)^{RM} = \left[\varepsilon_f(f_n) - \varepsilon_g(f_n)\left(1 - \eta_p\right)\right]/\eta_p. \quad (10)$$

Dielectric permittivity value of the most gases ε_g lies in the range 1.00006 … 1.01 e.g., helium 1.0000605, dry air 1.000536 and bromomethane 1.01028 [36–38]. A search in scientific information sources revealed a shortage of convincing investigations on dependence of permittivity of gasses on frequency. Taking into account that the considered frequency range f_n = 10 Hz, 20 Hz, … , 327 680 Hz lies below the frequencies of infrared radiation ~300 GHz, the permittivity of gaseous phase is assumed to be constant $\varepsilon_g \approx$ const. for the mentioned frequencies.

The numerical value of permittivity of the gaseous phase was estimated as follows. At each PUR foams density ρ_f and frequency f_n of the spectrum the experimentally determined value of $\varepsilon_f(\rho_f)$ was substituted into the rule of mixture, Eq. (10), Then different values of ε_g = 1.020 = cont., 1.010 = const. and 1.001 = const. were subsequently assumed, substituted in Eq. (10) as well and the corresponding value of permittivity of monolithic PUR polymer $\varepsilon_p(f_n)^{RM}$ was calculated. The procedure was repeated for all values of densities of the produced and tested experimentally PUR foams. Then the average value of permittivity of monolithic PUR $\varepsilon_p{}^{aver}(f_n)^{RM}$ at each f_n and at each assumed value of ε_g was calculated, Tab. 3 and compared to the experimentally determined values $\varepsilon_p(f_n)^{exp}$.

Table 3: Permittivity of monolithic petrochemical PUR polymer, corresponding to different values of ε_g

Frequency ordeal number	$\varepsilon_p(f_n)^{exp}$	$\varepsilon_p{}^{aver}(f_n)^{RM}$ ε_g = 1.020	RD; %	$\varepsilon_p{}^{aver}(f_n)^{RM}$ ε_g = 1.010	RD; %	$\varepsilon_p{}^{aver}(f_n)^{RM}$ ε_g = 1.001	RD; %
1	3.474	2.954	15.0	3.106	10.6	3.243	6.6
2	3.460	2.943	14.9	3.095	10.5	3.232	6.6
3	3.452	2.930	15.1	3.082	10.7	3.219	6.7
4	3.441	2.921	15.1	3.073	10.7	3.210	6.7
5	3.432	2.907	15.3	3.059	10.9	3.196	6.9
6	3.424	2.900	15.3	3.052	10.9	3.189	6.9
7	3.416	2.888	15.4	3.040	11.0	3.177	7.0
8	3.408	2.877	15.6	3.029	11.1	3.166	7.1
9	3.400	2.867	15.7	3.020	11.2	3.157	7.2
10	3.391	2.857	15.7	3.009	11.3	3.146	7.2
11	3.380	2.844	15.9	2.996	11.4	3.133	7.3
12	3.369	2.831	16.0	2.983	11.4	3.120	7.4
13	3.358	2.818	16.1	2.970	11.5	3.107	7.5
14	3.345	2.801	16.3	2.953	11.7	3.090	7.6
15	3.329	2.776	16.6	2.928	12.0	3.065	7.9
16	3.310	2.743	17.1	2.895	12.5	3.032	8.4

The relative difference RD; % between the experimentally determined values $\varepsilon_p(f_n)^{exp}$ and the average values found from the rule of mixture $\varepsilon_p{}^{aver}(f_n)^{RM}$ can be calculated as

$$RD = \left[\varepsilon_p(f_n)^{exp} - \varepsilon_p{}^{aver}(f_n)^{RM}\right] / \varepsilon_p(f_n)^{exp}. \quad (11)$$

Numerical calculations showed that at $\varepsilon_g \leq 1.001$ the values of RD became less than 8.5%, Tab. 3. To determine ε_g more precisely further investigations, including experimental ones, would be necessary. The permittivity value of gaseous phase ε_g = 1.001 is used in further calculations. With permittivity of PUR

$\varepsilon_p(f_n)$ known and permittivity of gaseous phase estimated, it becomes possible to calculate $\varepsilon_f(f_n)$ at any frequency f_n and any foams' density:

$$\varepsilon_f(f_n) = \varepsilon_p(f_n)\rho_f/\rho_p + \varepsilon_g\left(1 - \rho_f/\rho_p\right). \tag{12}$$

3.4 Maxwell–Garnett Equation

To calculate the effective (Macroscopic) permittivity of heterogeneous media, it is assumed that (a) Mixture responds to electromagnetic excitation as if it is homogeneous and (b) Size of the gaseous inclusions in the polymeric environment and the spatial correlation length of the permittivity function is small with respect to the wavelength. For the foams considered, the dimensions of typical polymeric structural elements and gaseous inclusions are in the limits 0.1–0.001 mm. The wavelength at the highest applied frequency f_{16} is $\lambda_{16} \approx 915$ m, thus the low-frequency character of the effective-medium model is in force. Considering petrochemical PUR foams as environment of monolithic PUR matrix with spherical gaseous inclusions with $\varepsilon_i \approx$ const., the effective permittivity ε_f of the mixture can be expressed according to Maxwell–Garnett equation [27] as:

$$\varepsilon_f(f_n) = \varepsilon_e(f_n) + \frac{3\eta_i\varepsilon_e(f_n)[\varepsilon_i - \varepsilon_e(f_n)]}{[\varepsilon_i + 2\varepsilon_e(f_n) - \eta_i(\varepsilon_i - \varepsilon_e(f_n))]}, \tag{13}$$

where ε_e and ε_i—permittivity of environment and inclusions; η_e and η_i—volume fractions of environment and inclusions; $\eta_i = 1.0 - \eta_e$. When $\eta_i \to 0.0$, $\varepsilon_f(f_n) \to \varepsilon_e(f_n)$ and when $\eta_i \to 1.0$, $\varepsilon_f(f_n) \to \varepsilon_i$.

Curves (a), (b) and (c) in Fig. 14 depict the effective permittivity of a theoretical heterogeneous media in dependence of volume fraction of environment η_e calculated according to Eq. (13) when permittivity of environment ε_e is (a) 1.0, (b) 2.0 and (c) 3.0 and permittivity of gaseous inclusions $\varepsilon_i \approx 1.00059$ (Air). For similar permittivity of environment ε_e and inclusions ε_i the effective permittivity of the composite is a nearly linear function of the volume fraction of inclusions and becomes an expressed nonlinear function for large dielectric contrasts. In case when permittivity of inclusions is lower than that of the environment $\varepsilon_i < \varepsilon_e$, the parameter of dielectric contrast $c = \varepsilon_i/\varepsilon_e \leq 1.0$. Curves (d) and (e) correspond to effective permittivity of a PUR composite—PUR foams, consisting of PUR environment with inclusions of gaseous phase, when $\varepsilon_e = \varepsilon_p = 3.474$ at frequency f_1 and $\varepsilon_e = \varepsilon_p = 3.310$ at f_{16}; $\varepsilon_i \approx 1.001$ for the gaseous phase. The parameter $c = \varepsilon_i/\varepsilon_e \approx 1.001/3.474 = 0.288 < 1.0$ at f_1 and $c = 1{,}001/3.310 = 0.302 < 1.0$ at f_{16}.

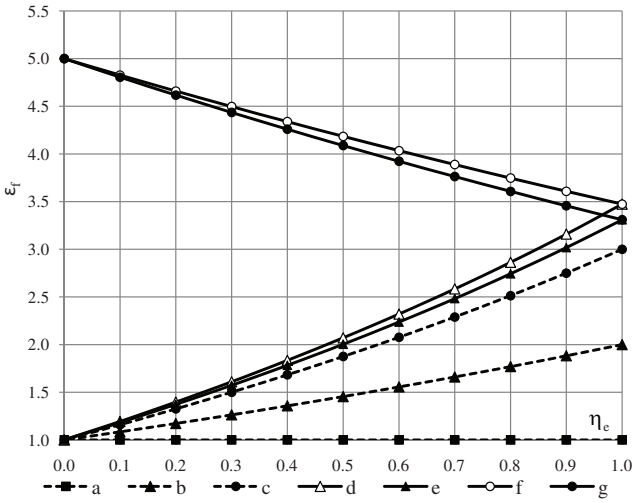

Figure 14: Effective permittivity of heterogeneous media

For comparison graphs (f) and (g) show effective permittivity of a PUR composite, consisting of a PUR environment filled with inclusions of higher permittivity $\varepsilon_i > \varepsilon_e$ (e.g., chopped short quartz fibers): $\varepsilon_i = 5.0$; $c = \varepsilon_i/\varepsilon_e \approx 5.0/3.47 = 1.439 > 1.0$ at f_1 and $c = 5.0/3.310 = 1.511 > 1.0$ at f_{16}.

3.5 Lichtenecker Equation

In [17] polystyrene foams and in [24] rigid PUR foams are considered as a statistic mixture of polymer and gas components and Lichtenecker equation is suggested for calculation of effective permittivity:

$$\varepsilon_f = \prod_{k=1}^{K} \varepsilon_k^{\eta_k}.$$

When the number of components K = 2, then

$$\varepsilon_f = \varepsilon_1^{\eta_1} \varepsilon_2^{\eta_2} = \varepsilon_p^{\eta_p} \varepsilon_g^{\eta_g}. \tag{14}$$

Figs. 15a and 15b presents effective permittivity of PUR foams calculated according to the rule of mixture, Maxwell–Garnett equation and Lichtenecker equation at $f_1 = 10$ Hz and $f_{16} = 0.33$ MHz for the whole range of space filling coefficient $0.0 \leq \eta_p \leq 1.0$.

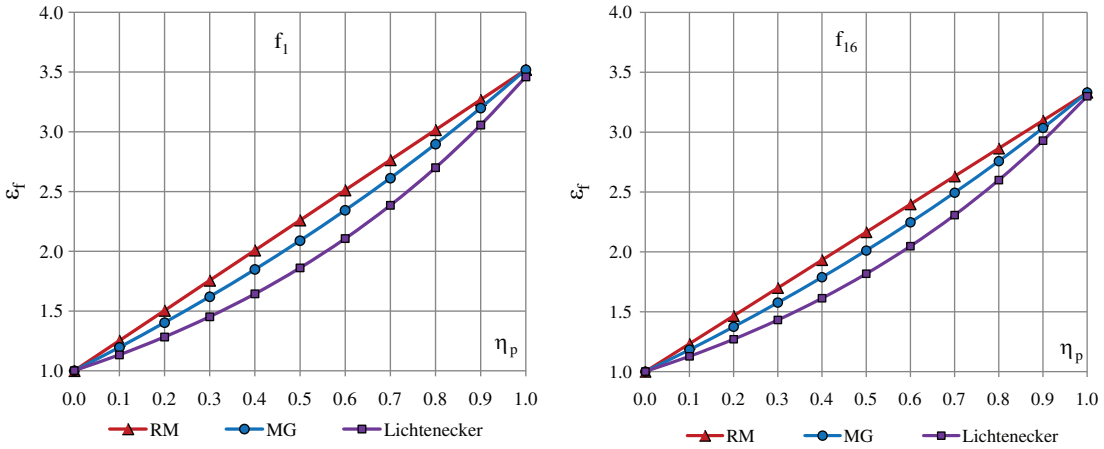

Figure 15: Effective permittivity of PUR foams at (a) f_1 and (b) f_{16}

Fig. 16 gives the same for frequencies (a) f_1 and (b) f_{16}, together with experimental data of Tab. 1 petrochemical PUR foams and the trendlines up to the value space filling coefficient $\eta_p \approx 0.43$. It can be seen that experimental data points are situated between the boundaries defined by the rule of mixture (Upper boundary) and Maxwell–Garnett equation (Lower boundary). The permittivity values according to Lichtenecker equation are ≈ 30–50% smaller than the experimentally determined ones and as such are not well fitted to describe experimental data of Tab. 1 petrochemical PUR foams, *Sika JSC* and *General Plastics Manufacturing Co*. PUR foams (Fig. 12).

4 Discussion

Dielectric permittivity of rigid, Latvia-grown rapeseed oil polyol PUR biofoams and petrochemical PUR foams was investigated for the first time in dependence of foams' density with a non-destructive dielectric spectrometer equipped with a capacitive sensor of one-side access type, at low frequencies 10, 20, …, 327 680 Hz. The acquired permittivity values are in a good correspondence with the experimental data in [24,25]. Permittivity of corresponding monolithic polyurethanes was determined as well.

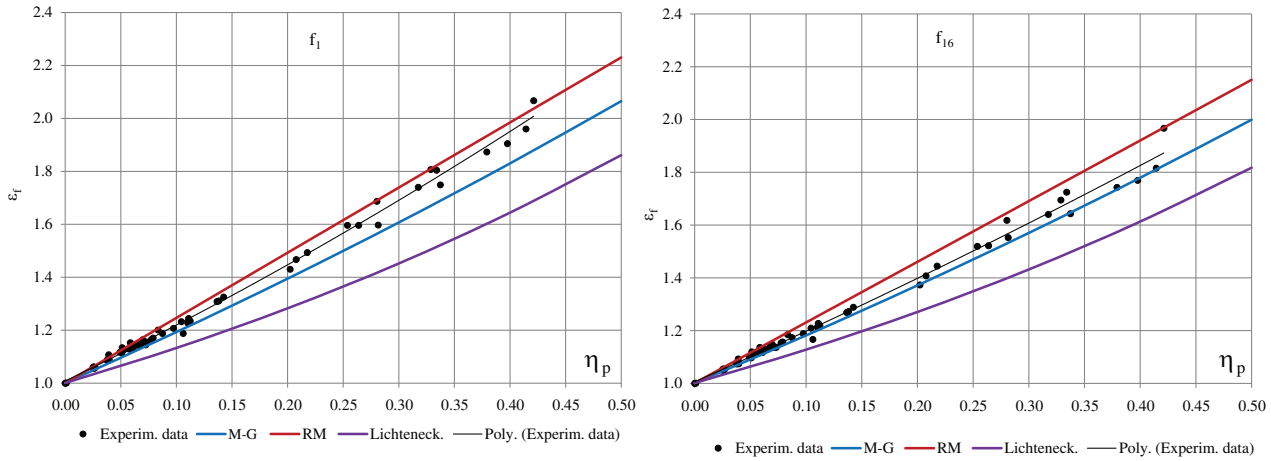

Figure 16: The calculated effective permittivity and experimental data; at (a) f_1 and (b) f_{16}

Permittivity of petrochemical PUR foams and PUR biofoams was compared with permittivity of PUR foams from European and American industrial producers *Sika JSC* and *General Plastics Manufacturing Co*. Experimental data proved that PUR foams of the Tab. 1 formulation exhibit dielectric permittivity, not exceeding that of the PUR foams from industrial producers: petrochemical PUR foams up to 550 kg/m^3 and PUR biofoams, comprising the renewable, Latvia grown rapeseed oil polyol in ready foams 27 wt.%–29 wt.%, up to densities 230–250 kg/m^3. That is a promising result for the countries, lacking petrochemical resources. At densities above 250 kg/m^3 presence of biopolyol in foams formulation may cause changes in cellular structure that increase the value of permittivity.

A comparison with experimental data of permittivity of PUR biofoams, petrochemical foams and both monolithic PUR-s, acquired with another apparatus/method—the *Novocontrol* Broadband Dielectric Spectrometer BDS-50 was made. The spectrometer is one of the most accurate devices presently in the market. It was determined that the relative difference between the data according to *Novocontrol* spectrometer and the data, measured with the OSA capacitive sensor [18,23] was less than ≈ 5% for petrochemical PUR foams of densities 95 and 222 kg/m^3.

Considering PUR foams as a heterogeneous media "Polymer—gaseous phase", the rule of mixture, Maxwell–Garnett equation and Lichtenecker equation [26,27,24] were used to describe mathematically the dependence of effective dielectric permittivity on the volume fraction of phases. The majority of experimental data points is situated between the boundaries determined by the rule of mixture (Upper) and Maxwell–Garnett equation (Lower). It was showed that Maxwell–Garnett matrix model provides considerably better results for calculation of effective permittivity of rigid PUR foams than the statistic mixture model and Lichtenecker equation.

The proposed OSA capacitive sensor method could find commercial applications in a portable multi-functional tester for non-destructive quality evaluation of PUR biofoams and petrochemical PUR foams. Such a tester is awaited for in on-spot evaluations, diagnostication and repair of PUR biofoams and petrochemical PUR foams in buildings, structures, protective radomes, aircrafts and space vehicles, ships, refrigerator vans, automobiles etc.

5 Conclusions

The following main conclusions were made:

1. For the experimentally determined permittivity spectra of petrochemical PUR foams, density 32.1–539.2 kg/m^3, permittivity values lie in the limits $1.059 \leq \varepsilon_f \leq 2.067$. For the experimentally determined

permittivity spectra of Latvia-grown rapeseed oil polyol PUR biofoams, density 81.2–442.4 kg/m^3, permittivity values lie in the limits $1.130 \leq \varepsilon_f \leq 2.003$. Dependence "Permittivity—density" at each frequency can be well approximated by a second order polynomial.

2. A technology for obtaining monolithic petrochemical-origin PUR and biopolyurethane in ampoules of inner diameter 25.4 mm was developed. Permittivity spectra of both types of monolithic polyurethane were determined experimentally, the permittivity values lying in the limits $3.474 \geq \varepsilon_p \geq 3.310$ and $3.413 \geq \varepsilon_{pb} \geq 3.100$. Permittivity value of the gaseous phase in closed-cell foams was estimated to be $\varepsilon_g \approx 1.001$ that corresponds to the values, characteristic for the most of gases. Knowledge about permittivity of components is urgently required in mathematical modeling and calculations of effective properties of "Polymer—gas" composite materials.
3. Up to densities 400–450 kg/m^3 the value of dropping factor of both types of the investigated PUR foams does not exceed ≈ 5.5%. PUR biofoams, comprising the rapeseed oil polyol, exhibit a dropping factor only ≈ 0.5%–1.0% higher that the petrochemical ones. For monolithic petrochemical polyurethane value of dropping factor is ≈ 6% and for biopolyurethane ≈ 7%.
4. Considering PUR foams as a heterogeneous media "Polymer—gaseous phase", the applicability of the rule of mixture and Maxwell–Garnett equation to model mathematically the dependence of effective dielectric permittivity on the volume fraction of phases was showed.

Acknowledgement: The research was performed in the European Regional Development Fund project No. 1.1.1.1/16/A/008 *"Development of multi-functional tester for non-destructive quality testing of materials and structures from rigid cellular plastics"*. Authors who received the grant: Ilze Beverte, Vairis Shtrauss, Aldis Kalpinsh and Uldis Lomanovskis. URL to sponsors' website: https://www.cfla.gov.lv/en/

Funding Statement: The research was performed in the European Regional Development Fund project No. 1.1.1.1/16/A/008. URL to sponsors' website: https://www.cfla.gov.lv/en/.

Conflicts of Interest: The authors declare that they have no conflicts of interest to report regarding the present study.

References

1. Hilyard, N. C. (1982). *Mechanics of cellular plastics*. New York: MacMillan.
2. Klempner, D., Frisch, K. C. (1991). *Handbook of polymeric foams and foam technology*. Munich: Hanser Publishers.
3. Montero de Espinosa, L., Meier, M. A. R. (2011). Plant oils: the perfect renewable resource for polymer science? *European Polymer Journal, 47(5),* 837–852. DOI 10.1016/j.eurpolymj.2010.11.020.
4. Stirna, U., Fridrihsone-Girone, A., Lazdina, B., Misane, M., Vilsone, D. (2013). Biobased polyurethanes from rapeseed oil polyols: structure, mechanical and thermal properties. *Journal of Polymers and the Environment, 21(4),* 952–962. DOI 10.1007/s10924-012-0560-0.
5. Petrovič, Z. S. (2008). Polyurethanes from vegetable oils. *Polymer Reviews, 48(1),* 109–155. DOI 10.1080/15583720701834224.
6. Kirpluks, M., Cabulis, U., Kurańska, M., Prociak, A. (2013). Three different approaches for polyol synthesis from rapeseed oil. *Key Engineering Materials, 559,* 69–74. DOI 10.4028/www.scientific.net/KEM.559.69.
7. Jumat, S., Saliha, N., Yousif, E. (2012). Industrial development and applications of plant oils and their biobased oleochemicals. *Arabian Journal Chemistry, 5(2),* 135–145. DOI 10.1016/j.arabjc.2010.08.007.
8. Caillol, S., Desroches, M., Boutevin, G., Loubat, C., Auvergne, R. et al. (2012). Synthesis of new polyester polyols from epoxidized vegetable oils and biobased acids. *European Journal of Lipid Science and Technologies, 114(12),* 1447–1459. DOI 10.1002/ejlt.201200199.

9. Vasconcelos Vieira Lopes, R., Loureiro, N. P. D., Pezzin, A. P. T., Gomes, A. C. M., Resck, I. S. et al. (2013). Synthesis of polyols and polyurethanes from vegetable oils-kinetic and characterization. *Journal of Polymer Research, 20(9),* 238–247. DOI 10.1007/s10965-013-0238-x.
10. Hu, S., Luo, X., Li, Y. (2014). Polyols and polyurethanes from the liquefaction of lignocellulosic biomass. *ChemSusChem, 7(1),* 66–72. DOI 10.1002/cssc.201300760.
11. Vale, M., Mateus, M. M., Dos Santos, R. G., Castro, C. N., Schrijver, A. et al. (2019). Replacement of petroleum-derived diols by sustainable biopolyols in one component polyurethane foams. *Journal of Cleaner Production, 212,* 1036–1043. DOI 10.1016/j.jclepro.2018.12.088.
12. Stirna, U., Cabulis, U., Beverte, I. (2008). Water blown polyisocyanurate foams from vegetable oil polyols. *Journal of Cellular Plastics, 44(2),* 139–160. DOI 10.1177/0021955X07084705.
13. Kuranska, M., Prociak, A., Kirpluks, M., Cabulis, U. (2013). Porous polyurethane composites based on bio-components. *Composites Science and Technology, 75,* 70–76. DOI 10.1016/j.compscitech.2012.11.014.
14. Prociak, A., Kuranska, M., Malevska, E. (2017). Porous polyurethane plastics synthetized using bio-polyols from renewable raw materials. *Polimery, 62(05),* 353–363. DOI 10.14314/polimery.2017.353.
15. Cabulis, U., Sevastyanova, I., Andersons, J., Beverte, I. (2014). Rapeseed oil-based rigid polyisocyanurate foam modified with nanoparticles of various type. *Polimery, 59(3),* 207–212. DOI 10.14314/polimery.2014.207.
16. Kremer, F., Schonhals, A. (2003). *Broadband dielectric spectroscopy.* Berlin, Heidelberg: Springer-Verlag.
17. Matiss, I. (1982). *Capacitive transducers for nondestructive testing*. Riga: Publishing House "Zinatne".
18. Kalpinsh, A., Shtrauss, V., Lomanovskis, U. (2013). Capacitive probe for non-destructive testing of dielectric materials. Patent: Patent Office of Republic of Latvia, 9, LR-1169.
19. Hu, X., Yang, W. (2010). Planar capacitive sensors—designs and applications. *Sensor Review, 30(1),* 24–39. DOI 10.1108/02602281011010772.
20. Nassr, A. A., Ahmed, W. H., El-Dakhakhni, W. W. (2008). Coplanar capacitance sensors for detecting water intrusion in composite structures. *Measurement Science and Technology, 7(19),* 1–7.
21. Gao, X., Zhao, Y., Ma, H. (2018). Fringing electric field sensors for anti-attack at system-level protection. *Sensors, 18(9),* 3034. DOI 10.3390/s18093034.
22. Chang, X. M., Dou, Y., Zhuo, D., Fan, J. H. (2012). Research on sensor of ice layer thickness based on effect of fringe electric field. *Proceedings of the 2012 International Conference on Computing, Measurement, Control and Sensor Network,* pp. 417–420, Taiyuan, China.
23. Kalpinsh, A., Shtrauss, V., Lomanovskis, U. (2019). Digital emulation of dielectric relaxation functions for capacitive sensors of non-destructive dielectric spectrometry. *Computational Methods and Experimental Measurements, XIX PI,* 111–119, *https://www.witpress.com/Secure/elibrary/papers/CMEM19/CMEM19011FU1.pdf*.
24. Traeger, M. K. (1967). Physical properties of rigid polyurethane foams. *Journal of Cellular Plastics, 3(9),* 405–418. DOI 10.1177/0021955X6700300906.
25. Domeier, L., Hunter, M. (1999). Epoxy foam encapsulants: processing and dielectric characterization. *https://prod.sandia.gov/techlib-noauth/access-control.cgi/1999/998213.pdf*.
26. Richardson, M. O. W. (1977). *Polymer engineering composites*. London: Applied Science Publishers Ltd.
27. Sihvola, A. (2000). Mixing rules with complex dielectric coefficients. *Subsurface Sensing Technologies and Applications, 1(4),* 393–415. DOI 10.1023/A:1026511515005.
28. Kurańska, M., Prociak, A., Kirpluks, M., Cabulis, U. (2015). Polyurethane-polyisocyanurate foams modified with hydroxyl derivatives of rapeseed oil. *Industrial Crops and Products, 74,* 849–857. DOI 10.1016/j.indcrop.2015.06.006.
29. Fridrihsone, A., Stirna, U., Lazdina, B., Misane, M., Vilsone, D. (2013). Characterization of polyurethane networks structure and properties based on rapeseed oil derived polyol. *European Polymer Journal, 49(6),* 1204–1214. DOI 10.1016/j.eurpolymj.2013.03.012.
30. Renz, R. (1977). *Zum zuegigen und zyklischen verfomungsverhalten polymerer hartschaumstoffe (dissertation zur erlangung des grades doktor-ingenieur)*. Universität Karlsruhe (TH), Deutschland.

31. Beverte, I. (2014). Determination of highly porous plastic foams' structural characteristics by processing LM images data. *Journal of Applied Polymer Science, 131(4),* 39477. DOI 10.1002/app.39477.
32. Hawkins, M. C., O'Toole, B., Jackovich, D. (2005). Cell morphology and mechanical properties of rigid polyurethane foam. *Journal of Cellular Plastics, 41(3),* 267–285. DOI 10.1177/0021955X05053525.
33. Venkatesh, M. S., Raghavan, G. S. V. (2005). An overview of dielectric properties measuring techniques. *Canadian Biosystems Engineering, 47*.
34. Chen, T. (2012). *Capacitive sensors for measuring complex permittivity of planar and cylindrical structures (A dissertation)*. Iowa State University, Capstones. https://lib.dr.iastate.edu/etd/12294.
35. Matiss, I. (2014). Multi-element capacitive sensor for non-destructive measurement of the dielectric permittivity and thickness of dielectric plates and shells. *NDT & E International, 66,* 99–105. DOI 10.1016/j.ndteint.2014.05.003.
36. Clarke, R. N. (2006). *Dielectric properties of materials*. http://www.kayelaby.npl.co.uk/general_physics/2_6/2_6_5.html.
37. Hill, N. E., Vaughan, W. E., Price, A. H., Mansel, D. (1969). *Dielectric properties and molecular behaviour.* London: Van Nostrand Reinhold Company Ltd.
38. Brodie, G., Mohan, V. J., Farrell, P. (2015). *Microwave and radio-frequency technologies in agriculture*. https://www.degruyter.com/view/product/466435.